

Crack-EdgeSAM: Self-Prompting Crack Segmentation System for Edge Devices

Yingchu Wang, Ji He, Shijie Yu

Abstract—Structural health monitoring (SHM) is essential for the early detection of infrastructure defects, such as cracks in concrete bridge pier, but often faces challenges in efficiency and accuracy in complex environments. Although the Segment Anything Model (SAM) achieves excellent segmentation performance, its computational demands limit its suitability for real-time applications on edge devices. To address these challenges, this paper proposes Crack-EdgeSAM, a self-prompting crack segmentation system that integrates YOLOv8 for generating prompt boxes and a fine-tuned EdgeSAM model for crack segmentation. To ensure computational efficiency, the method employs ConvLoRA, a Parameter-Efficient Fine-Tuning (PEFT) technique, along with DiceFocalLoss to fine-tune the EdgeSAM model. Our experimental results on public datasets and the climbing robot automatic inspections demonstrate that the system achieves high segmentation accuracy and significantly enhanced inference speed compared to the most recent methods. Notably, the system processes 1024 x 1024 pixels images at 46 FPS on our PC and 8 FPS on Jetson Orin Nano.

Index Terms—Crack segmentation, Segment Anything, YOLOv8, Parameter-Efficient Fine-Tuning, climbing robots, edge devices.

I. INTRODUCTION

IN the field of defect prevention, structural health monitoring (SHM) is a crucial method for protecting infrastructure such as roads and bridges by detecting potential structural collapse and physical damage [1]. To overcome the high costs and low efficiency of traditional SHM methods [2], an increasing number of advanced computer vision-based technologies have been developed and implemented in automatic assessment. The application of computer vision techniques to SHM, particularly for defects pixel-level detection (segmentation), has been researched for decades. The exploration primarily follows two branches: traditional image-processing methods and neural network-based methods.

In the field of image processing, the traditional crack detection approaches could be classified into histograms, morphology, filtering and model analysis [3]. For instance, there is one method that utilizes continuous wavelet transform (CWT) for pavement crack detection [4], while another approach uses a steerable matched filter (a filtering method) combined with crack features and contours to identify cracks at pixel-level [5]. However, these methods lack semantic understanding, which limits their performance in challenging scenarios, such as input data with complex photometric characteristics, cluttered backgrounds, and noise. Deep learning-based methods have ad-

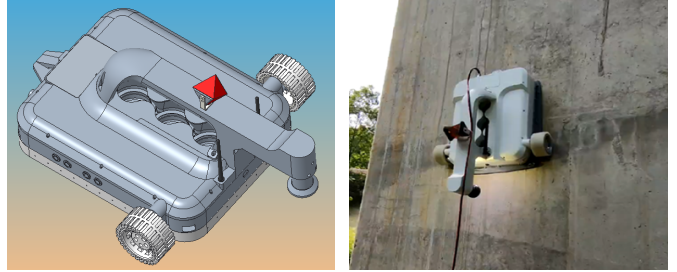


Fig. 1. (a) The climbing robot model in the SolidWorks. (b) The climbing robot executed an inspection task on a concrete bridge pier.

vanced the field significantly. In 2017, Reference [6] proposed CrackNet, an unconventional CNN model that removes max pooling layers to ensure pixel-level segmentation accuracy. Reference [7] proposed a novel CNN architecture (SDDNet) for SHM, composed of a specially designed encoder-decoder module with an enhanced ASPP (Atrous Spatial Pyramid Pooling). References [8] and [9] explored the feasibility of U-Net, a convolutional neural network that leverages multi-level feature fusion, in pavement crack segmentation. Additionally, to achieve zero-shot capability in models, recent efforts have focused on a foundation model, the Segment Anything Model (SAM). Although SAM approaches have demonstrated effectiveness in the detection of defects, the learning step is expensive [3]. To enhance the efficiency of training, reference [10] and [11] propose fine-tuned SAM models by using Low-Rank Adaptation (LoRA). Similar to the significant impact SAM has had in fields, such as medical imaging, agriculture, and manufacturing, the fine-tuned SAM model offers substantial advantages for structural health monitoring [12].

Furthermore, image-based visual inspection approaches are usually equipped on low-cost autonomous platforms, to demonstrate the capability of approaches in real-world tasks. For instance, Reference [13] combines a traditional image processing method with an obstacle-avoidance algorithm to propose a UAV-based monitoring system. Subsequently, Reference [2] implements automatic damage detection for UAVs using a designed CNN model and geo-tagging methods for localization. In the field of vertical structures, references [14] and [15] demonstrate the capability of climbing robots with magnetic adhesion on steel structures, and [15] integrates traditional image processing methods to detect defects and stitch collected images. For no ferromagnetic surfaces, such as concrete bridge piers, wheeled robots with negative pressure adhesion are a commonly used combination [16]. Reference [17] presents a climbing robot inspection system that integrates

The climbing robot is owned by Shanghai Guimu Robot Company, Ltd., Shanghai, China.

Yingchu Wang (e-mail)

a VINS (visual-inertial navigation system) navigation module and a CNN-based defect classification module.

Inspired by these studies, this paper introduces a novel defects detection system, Crack-EdgeSAM, a self-prompting crack segmentation system, and implemented on a climbing robot platform (see Fig. 1). Our system integrates YOLOv8 and fine-tuned EdgeSAM, the YOLOv8 model generates crack bounding boxes as prompts for the EdgeSAM model, and then EdgeSAM segments the cracks based on the input image and prompts. This enables the climbing robot to obtain real-time crack segmentation results during the execution of the inspection task. Additionally, we briefly introduce the robot system in the section of Methodology, to explain how the robot achieves positioning, navigation and data collection, thereby demonstrating the feasibility of our method in real-world inspection tasks.

The main contributions of this paper can be summarized as follows:

- 1) We propose a novel climbing robot system for SHM of bridges. In this system, the robot has the capability to autonomously complete inspection tasks and can perform real-time crack detection and segmentation on the captured images during the bridge surface inspection.
- 2) A self-prompting segmentation system is designed, which can automatically generate prompt boxes and segment cracks in real-time.
- 3) A lightweight Segment Anything Model is introduced to achieve efficient and accurate crack segmentation on edge devices. To the best of our knowledge, our model is the first work to fine-tune EdgeSAM using ConvLoRA (PEFT technology) and DiceFocalLoss for real-time crack segmentation.
- 4) A loss function-related experiment demonstrates the effectiveness of DiceFocalLoss. Experiments on Khanhha [18] 's test dataset and the real-world dataset demonstrate that the proposed system performs comparably to state-of-the-art methods while achieving a higher inference speed.

II. RELATED WORK

Crack segmentation is a widely researched topic in the field of structural health monitoring (SHM). Due to the significant differences between crack images and natural images, achieving rapid and accurate crack segmentation could be a considerable challenge. CNN-based methods, such as CrackNet [6], SDDNet [7], CrackU-net [8] and CrackW-net [9], have led to substantial progress in this field. However, considering the interference factors in practical implementations, the research on SAM-based crack segmentation methods shows a better performance, especially its zero-shot capability. The methods mainly include a fine-tuning SAM [10] and CrackSAM [11], demonstrating high segmentation accuracy across various scenarios. Despite the remarkable performance of SAM-based models in real-world tasks, their high computational resource requirements make them difficult to deploy on edge devices for real-time segmentation. Fully training a large-scale foundational model is a resource-intensive process. In order to reduce training costs, a common approach is to employ PEFT methods for model fine-tuning. Ye et al. [10] provide a

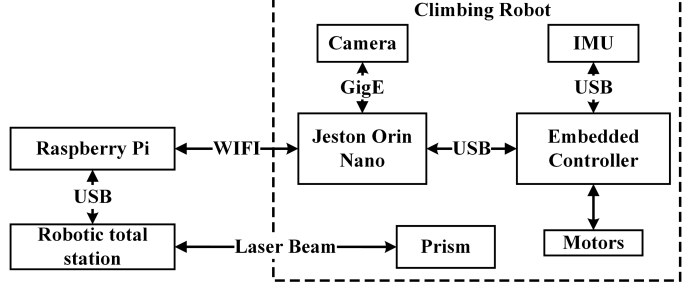


Fig. 2. The climbing robot system using robotic total station and trackable prism.

comprehensive review of fine-tuning SAM through Parameter-Efficient Fine-Tuning (PEFT) approaches, categorizing them into two classes, fine-tuning lightweight mask decoder of SAM [19], and adding additional layers to the original SAM model, such as various lightweight adapters [20] [21], LoRA-based methods [22] [23] [24] [25]. The parallel structure design of LoRA and the implementation of the linear fine-tuning matrices ensure inference efficiency and could be easily integrated into the original projection matrix. Therefore, LoRA-based methods are widely used for fine-tuning SAM models in medical and concrete crack segmentation downstream tasks.

Self-prompting is a common method that can automatically detect the prompts required by the SAM model from the input image. It replaces the manual input of prompts during the interactive procedures and enhances the level of automation in object segmentation substantially. Mobina et al. [26] demonstrated that combining YOLOv8's bounding box predictions with SAM achieves high segmentation accuracy while significantly reducing annotation time.

III. METHODOLOGY

A. Climbing Robot System

1) *Robot Design:* The robot's adhesion and locomotion mechanisms are similar to those of conventional pneumatic adhesion climbing robots [16] [27]. It uses electrical vacuum generators and a simple differential drive system for adhesion and movement, with a tail-mounted caster wheel and a sealed chamber providing stability. For image acquisition, an industrial camera with a resolution of 3200×2000 is mounted on the top bracket. A fully reflective prism is installed for real-time tracking during inspection tasks, and its position is indicated as the red component in the left image of Fig. 1.

2) *System Design:* To develop an autonomous image acquisition robot for the inspection of vertical structure, the architecture of the climbing robot system is shown in Fig. 2. Inspired by UAV-based inspection systems [28] [29], our framework primarily leverages a Topcon's robotic TS (total station) and an industrial camera to achieve fully covered automatic crack detection in the working area. In the particular implementation of the inspection task, the inspected area and the corresponding coordinate are initialized by the Total Station. Then, the global path planner generates a full coverage path of the working area and sends it to the robot via WI-FI. The robot's EKF (Extended Kalman Filter) module calculates

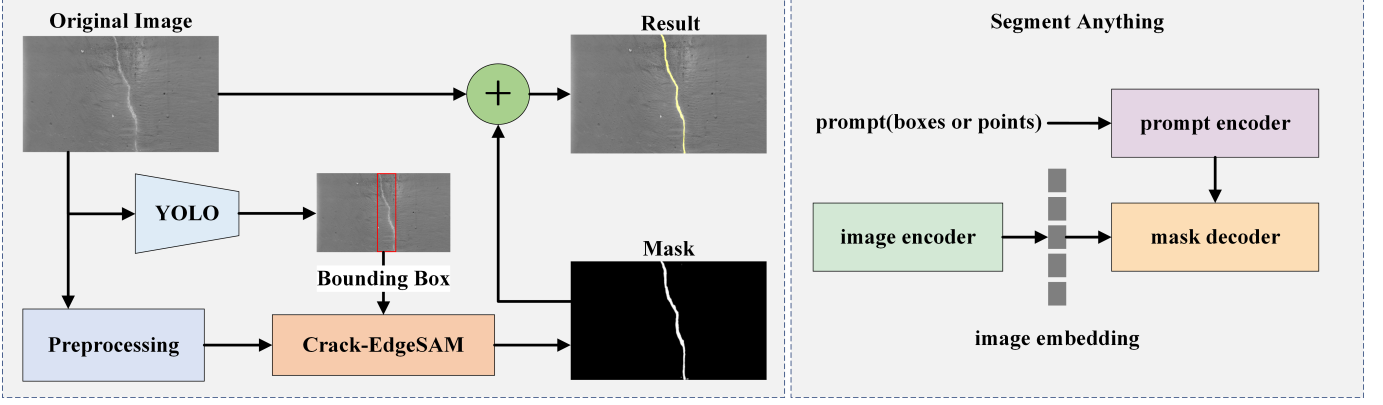


Fig. 3. The framework of self-prompts crack segmentation system with the architecture of Segment Anything Model (SAM). The preprocessing module resizes and pads the input original image, transforming it into a tensor with dimensions (1, 3, 1024, 1024) for the input of the Crack-EdgeSAM image encoder. The final result is obtained by computing the weighted sum of the original image and the mask image.

its pose using the global position provided by the TS and IMU data, while a PID control algorithm is employed to ensure the robot follows the predetermined trajectory.

Through this design, the robot achieves automated image-based inspection of vertical concrete bridge surfaces. The collected data supports the validation of the self-prompts crack segmentation system in real-world scenarios.

B. Self-prompts Crack Segmentation System

1) *Preliminary*: Segment Anything Model (SAM) is an efficient and promotable zero-shot model for image segmentation. As the overview shown in Fig. 3, the SAM model contains three modules: image encoder, prompt encoder and mask decoder [30]. The image encoder is responsible for converting the input high-resolution image into an embedding by using a pre-trained ViT-based (Vision Transformer) model. The prompt encoder utilizes sparse or dense prompts, including points, boxes, text and masks to generate prompt embeddings. These embeddings (image and prompts) and output tokens are mapped to masks and IoU scores by the lightweight mask decoder. Through this innovative and sophisticated design, the SAM model achieves exceptional precision in the tasks of interactive segmentation. Furthermore, as a foundational model, SAM has been strictly evaluated on images that were not included in the SA-1B (the dataset includes 1B masks from 11M images), and the results of zero-shot transfer experiments suggest that the model is capable of handling a variety of segmentation tasks [30].

The lightweight version of SAM models, such as FastSAM [31], EdgeSAM [32] and MobileSAM [33], enable the possibility of real-time processing on edge devices for the original SAM model. FastSAM optimizes the image encoding component by replacing the original module with a more computationally efficient CNN-based detector, which has fewer parameters and is easier to compute [31]. In addition, MobileSAM and EdgeSAM are inspired by the method of knowledge distillation to obtain a lightweight image encoder. In this work, we select the EdgeSAM as the segmentation module, due to its remarkable performance [32] [33].

Inspired by UAV-based inspection systems [28] [29], our framework primarily leverages a Topcon's robotic TS (total station) and an industrial camera to achieve fully covered automatic crack detection in the working area. In the particular implementation of the inspection task, the inspected area and the corresponding coordinate are initialized by the Total Station. Then, the global path planner generates a full coverage path of the working area and sends it to the robot via WI-FI. The robot's EKF (Extended Kalman Filter) module calculates its pose using the global position provided by the TS and IMU data, while a PID control algorithm is employed to ensure the robot follows the predetermined trajectory.

Through this design, the robot achieves automated image-based inspection of vertical concrete bridge surfaces. The collected data supports the validation of the self-prompts crack segmentation system in real-world scenarios.

2) *Crack Segmentation Workflow*: The proposed self-prompts crack segmentation system integrates two fundamental models, YOLO and SAM, to effectively detect and segment cracks in the automatic inspection tasks of the wall-climbing robot. The system follows a similar pipeline to common YOLO+SAM architecture [34], the SAM model utilizes the bounding boxes inferred by the YOLO model as inputs to SAM's prompt encoder, facilitating accurate segmentation of the target objects. For the box prompts generator, a pre-trained YOLOv8n model is employed for fast and accurate crack detection and output bounding boxes in real-time. These bounding boxes are fed into the prompt decoder of fine-tuned EdgeSAM, which enables the crack detection system's self-prompts functionality. The framework of the system is illustrated in Fig. 3.

C. EdgeSAM Fine-tuned Method

1) *Adaptation Method*: Fine-tuning the large-scale foundational models is a common step for applying the model to a specific task, as this approach not only improves the model performance but also reduces the resource consumption associated with fully training the large model. Recently fine-tuned SAM-based segmentation projects, such as CrackSAM [11], leverage adapters and low-rank adaptation (LoRA) methods

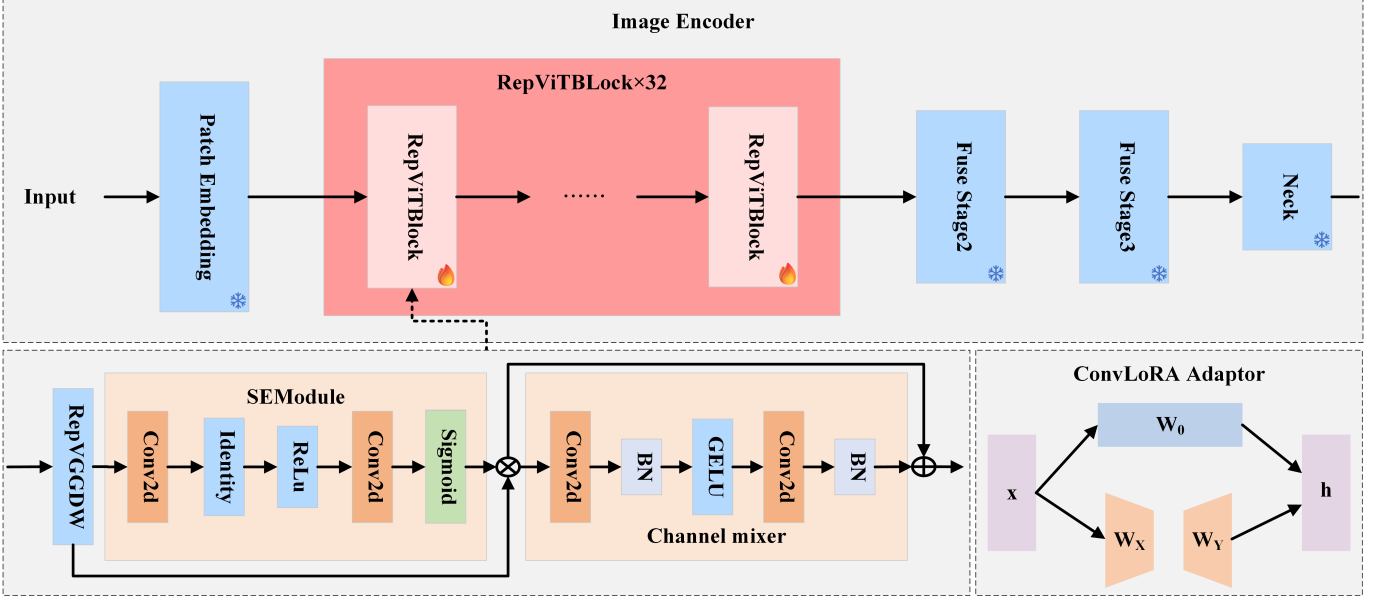


Fig. 4. The structure of EdgeSAM’s image encoder with trainable and frozen blocks. In the SEModule and Channel mixer, each convolutional layer is replaced with a ConvLoRA adaptor. In ConvLoRA Adaptor, W_0 represents the pre-trained weights of the convolutional layer, while W_X and W_Y are the low-rank weight matrices.

to fine-tune SAM, and achieve excellent performance of crack segmentation in various scenarios. Although the size of the parameters stored after fine-tuning is about 40MB, the 2.38GB size of the sam_vit_h_4b8939 could result in low.

To address the above issues, we propose a new fine-tuning approach for EdgeSAM. Considering the image encoder of EdgeSAM is distilled from the original Vit-based SAM encoder, the common strategies for fine-tuning SAM by using LoRA may no longer be applicable. Inspired by ConvLoRA [11] [35], we propose an effective fine-tuning method for EdgeSAM that enables it to achieve good performance in the crack detection tasks of the climbing robot. Specifically, the image encoder of EdgeSAM is a CNN-based network obtained by distilling the original ViT-based SAM image encoder. In the fine-tuning of the EdgeSAM image encoder, only the weights of the convolutional layers in the SEModule and Channel mixer of RepViTBLOCKS are trained, while the Patch Embedding, Fuse Stages2 and 3, and Neck module are all frozen. For RepViTBLOCKS adaptation, the ConvLoRA method is implemented in the fine-tuning process, as shown in Fig. 4. ConvLoRA retains the core concept of LoRA, applying low-rank constraints through weight updates in convolutional layers, which makes it possible to achieve Parameter-Efficient Fine-Tuning (PEFT) of the neural network, the diagram of ConvLoRA adaptor is shown in Fig. 4. Mathematically, the equation of ConvLoRA could be defined as follows:

$$h = W_0x + W_XW_Yx \quad (1)$$

where $W_0 \in \mathbb{R}^{C_{out} \times C_{in}}$, $W_X \in \mathbb{R}^{rank \times C_{in}}$, $W_Y \in \mathbb{R}^{C_{out} \times rank}$, and x is the input tensor, $rank$ value is much smaller than the minimum of the input (C_{in}) and output (C_{out}) channel numbers. Besides the weights of W_X and W_Y are initialized with a random Gaussian distribution and zero, respectively. In the training process, W_0 is frozen only the W_X

and W_Y can receive updated gradients to train parameters. In the process of fine-tuning EdgeSAM, the ConvLoRA adaptors are integrated into the conv2d layers of SEModule and Channel mixer, as shown in Fig. 4. Through the experiments, the model shows the best performance of segmentation when $rank = 4$.

2) *Loss function*: For the task of segmentation, several loss functions could be used to quantify the difference between predictions and labels, such as DiceLoss, DiceCELoss (Cross-Entropy) and DiceFocalLoss. However, crack images differ from natural images in that their features are similar to medical images, with imbalances between foreground and background, as well as between easy and hard examples. Inspired by medical image segmentation and considering the imbalanced nature of the training dataset, we leverage DiceFocalLoss to address the imbalance problems mentioned above, thereby improving model performance. Focal loss is an effective method that can deal with the problem of class imbalance. According to the equation proposed in [36], a typical form of Focal Loss can be defined as:

$$\mathcal{L}_{FL} = FL(p_t) = -(1 - p_t)^\gamma \log(p_t) \quad (2)$$

$$p_t = \begin{cases} p, & \text{when } y = 1 \\ 1 - p, & \text{when } y = 0 \end{cases} \quad (3)$$

where $\gamma \geq 0$ is a tunable focusing parameter and set to 4 during training.

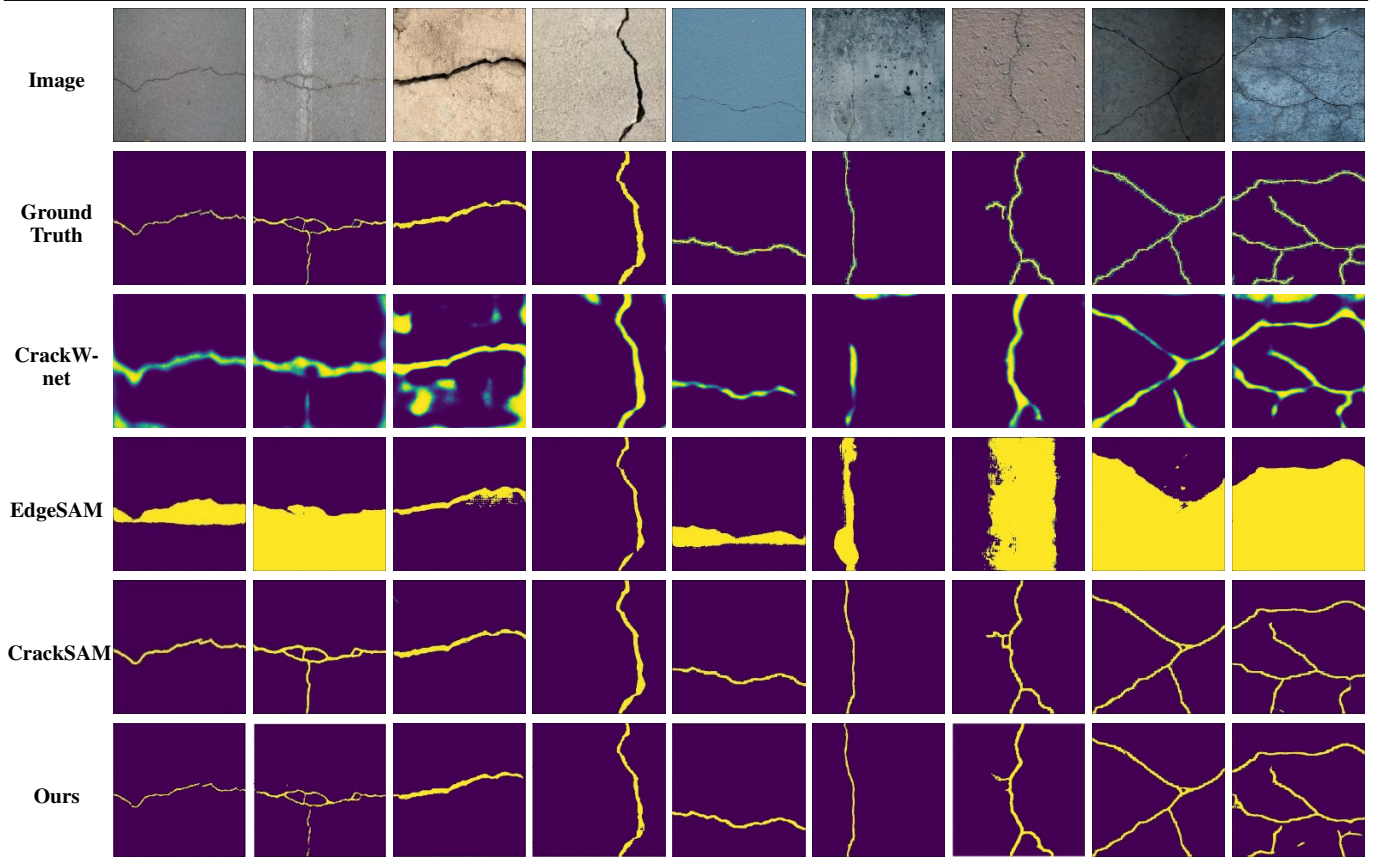
For Dice Loss, a loss function commonly used in image segmentation tasks, the input P is the binarized prediction and input G is the ground truth, the equation is as follows,

$$\mathcal{L}_{DL} = DL(P, G) = 1 - \frac{2 \sum_{i=1}^N p_i g_i}{\sum_{i=1}^N p_i^2 + \sum_{i=1}^N g_i^2} \quad (4)$$

where $p_i \in P [0, 1]$ and $g_i \in G [0, 1]$.

TABLE I

FINE-TUNED EDGESAM VISUALIZATION RESULT OF COMPARATIVE EXPERIMENTS ON KHANHHA'S [18] TEST DATASET WITH THREE OTHER DIFFERENT STATE-OF-THE-ART MODELS.



DiceFocalLoss combines Focal Loss (Eq. (2) and Dice Loss (Eq. (3)), with their respective functions shown below,

$$\mathcal{L}_{DFL} = \lambda_{DL}\mathcal{L}_{DL} + \lambda_{FL}\mathcal{L}_{FL} \quad (5)$$

where we set λ_{DL} to 0.8, λ_{FL} to 0.2. By hiring \mathcal{L}_{DFL} as the loss function, the performance of the model has been improved on the crack segmentation task, especially compared with DiceLoss and DiceCELoss.

IV. EXPERIMENTS AND RESULTS

A. Dataset

A dataset compiled by Khanhha [18] is utilized for fine-tuning the image encoder of the EdgeSAM model. The dataset integrates CRACK500 [37], GAPs384 [38], CFD [39], AEL [40], CrackTree [41], CrackForest [39] and DeepCrack [42], comprising 9,603 training images and 1,695 testing images, along with their corresponding masks, all with a resolution of 448×448 pixels. The dataset is employed for Crack-EdgeSAM, with the training set supporting parameter fine-tuning and loss function experiments, and the testing set enabling quantitative performance evaluation. Additionally, a real-world dataset, containing 759 images from Bridge A and 646 images from Bridge, each with a resolution of 3,000×2,000 pixels, is used to assess the zero-shot capability and performance of

the self-prompting crack segmentation system in real-world inspection scenarios. Notably, both 448×448 and 3000×2000 images are resized to a resolution of 1,024×1,024 pixels by the preprocessing module, as shown in Fig. 3.

B. Implementation Details

Our proposed approach consists of two parts: the lightweight fundamental model fine-tuning and segmentation performance evaluation on a GeForce RTX 4070Ti GPU platform, CrackEdgeSAM efficiency testing and real-world scenario experiments on a Jetson Orin Nano 8GB. For EdgeSAM fine-tuning, the image encoder of the model is processed using the ConvLoRA method mentioned in Chapter III, then trained for 100 epochs using the Adam optimizer with 1e-4 learning rate (no weight decay), and DiceFocalLoss is used as the loss function. In addition, due to the performance limitation of the GPU, the batch size is set to 4.

For the real-world experiment, the climbing robot executes an automatic data collection task on the bridge pier surface. During the process of inspection, the localization and navigation module guide the robot along the planned path, while the onboard camera captures images of the bridge surface. Finally, cracks in images are detected and marked by the self-prompting crack segmentation system.

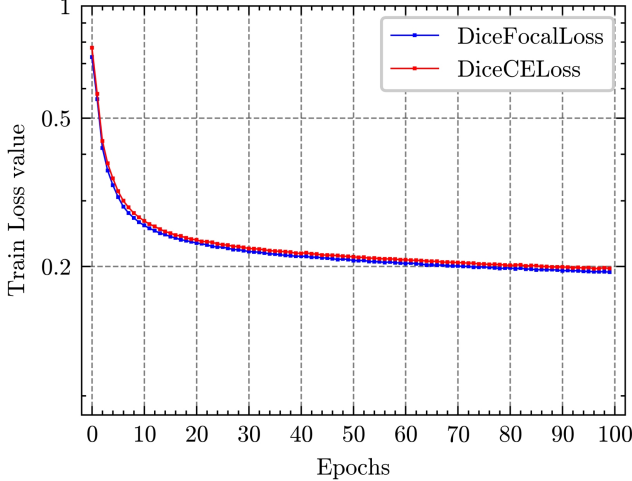


Fig. 5. Comparison of train loss value on different loss functions.

C. Experimental Results

1) *Loss Functions Comparison*: Fig. 5 shows the curves of the four loss functions on the training dataset. The green line represents DiceLoss, the red line represents DiceCELoss, and the blue line represents DiceFocalLoss. According to the result, DiceFocalLoss has a lower convergence value compared to other three loss functions after 100 epochs, the final loss values of the functions are 0.21976, 0.19737 and 0.17755 in the order of the legend on the Fig. 5. The train loss curves indicate that DiceFocalLoss performs excellently in training on the concrete crack dataset. Meanwhile, it demonstrates that DiceFocalLoss minimizes the impact of imbalance problems on the training process.

2) *Evaluation on Public Dataset*: TABLEI presents comparisons of crack segmentation results with SOTA methods on 1695 images, Khanhha's test dataset. We selected 9 images of cracks with different shapes on various concrete materials from the test dataset to depict the prediction results of different models. The input prompt of the model is the bounding boxes of the cracks' ground truth. In TABLEI, the first two rows of the table show the original image and the corresponding ground truth mask. The remaining rows display the segmentation results of CrackW-net [3], original EdgeSAM, CrackSAM, and CrackEdgeSAM, respectively. According to the third row of the table, CrackW-net shows low precision of the crack segmentation, it cannot capture the detailed structure of the cracks. The images in the fourth row of the table clearly show that the original EdgeSAM is unable to precisely segment images where the difference between cracks and the background is not prominent. CrackSAM and ours demonstrated extraordinary crack segmentation capabilities on the test dataset.

Refer to the metrics hired in [2], precision, recall, accuracy, and IoU are used to evaluate the performance of the models on the test dataset,

$$Precision = \frac{TP}{TP + FP} \quad (6)$$

TABLE II
PERFORMANCE COMPARISON ON DIFFERENT NETWORKS.

Networks	Precision	Recall	F1	IoU	FPS
CrackW-net	0.3261	0.6640	0.3889	0.2579	8.2372
EdgeSAM	0.1835	0.7645	0.2494	0.1575	63.4140
CrackSAM	0.7471	0.7718	0.7460	0.6086	14.5794
Ours (r=2)	0.7569	0.7027	0.7047	0.5578	63.3798
Ours (r=4)	0.7426	0.7377	0.7143	0.5685	63.2227
Ours (r=8)	0.7449	0.7201	0.7095	0.5625	62.3914
Ours (r=16)	0.7632	0.6974	0.7069	0.5602	61.4965

TABLE III
THE VISUALIZATION RESULT OF SELF-PROMPTING CRACK SEGMENTATION SYSTEM.

Image				
Ground Truth				
Ours				
IoU	0.5781	0.6074	0.6826	0.8035

$$Recall = \frac{TP}{TP + FN} \quad (7)$$

$$F1 = \frac{2 * TP}{2 * TP + FP + FN} \quad (8)$$

$$IoU = \frac{TP}{TP + FP + FN} \quad (9)$$

where TP is true positive, TN is true negative, FP is false positive, FN is false negative. Additionally, the average inference time of each image will be calculated as FPS. As the data shown in TABLEII, the original EdgeSAM couldn't segment cracks accurately, with a recall of 0.7645 and IoU of 0.1575, indicating that the model contains a significant number of false positives during the segmentation. For our fine-tuned model, we tested different rank values ranging from 2 to 16, and the model achieved the best segmentation performance, with an IoU of 0.5685, when the rank was set to 4. Through a comprehensive comparison of metrics between our method, CrackW-net and CrackSAM, our method shows a better performance than CrackW-net but has an IoU of approximately 0.04 lower than CrackSAM, however, in terms of the speed of segmentation. On the RTX 4070Ti platform,

TABLE IV
FINE-TUNED EDGESAM VISUALIZATION RESULT OF COMPARATIVE EXPERIMENTS ON KHANHHA'S [18] TEST DATASET WITH THREE OTHERS DIFFERENT STATE-OF-THE-OUT MODELS.

Image									
Ground Truth									
Ours									
IoU	0.4769	0.5405	0.6006	0.4881	0.6728	0.4169	0.4483	0.7059	0.7208

with CUDA acceleration, our model achieves an inference speed approximately 4.3 times faster than CrackSAM and 7.7 times faster than CrackW-net. The above comparison demonstrates that our model ensures the accuracy of crack segmentation while also achieving remarkable inference speed.

Moreover, we assess the performance of a self-prompting crack segmentation system using the test dataset. TABLEIII showcases the original images with bounding boxes detected by YOLOv8, the ground truth of cracks, and the segmentation results generated by Crack-EdgeSAM using the red bounding boxes as input prompts. In terms of efficiency, the system processes a 448*448 resolution testing image with an average used time of 0.0267ms (46.0829FPS). And the system's precision, recall, F1 score, and IoU are 0.7202, 0.6784, 0.6698, and 0.5204 respectively.

3) *The System's Performance on Climbing Robot:* In order to demonstrate the segmentation capability of Crack-EdgeSAM and its performance in practical applications, we experimented with automated inspection using the climbing robot on two different concrete bridge piers. The system's detection and segmentation results, along with the IoU values for the bridge inspection task, are presented in TABLEIV. In the table, the original images' red bounding boxes are generated by YOLOv8, and they will be used as prompts fed into fine-tuned EdgeSAM. In the experiments, we implemented our approach on the Nvidia Orin Nano platform and accelerated yolov8 and crack-EdgeSAM using TensorRT, enabling the system could detect and segment cracks in real time during the task. The input image with a resolution of 3000×2000 is preprocessed as a 1024×1024 image and transformed into a tensor with dimensions of (1, 3, 1024, 1024), which are fed into the Crack-EdgeSAM model with the rescaled box prompts. The average processing time for bounding boxes was 18.75ms, and for crack segmentation was 100.827ms.

TABLE V
PERFORMANCE COMPARISON ON DIFFERENT NETWORKS.

Networks	Total Params	Trainable Params	Input and Size	Params Size
Crack-EdgeSAM	5517552	46992	12.00MB	21.05MB

V. CONCLUSION

This paper introduces Crack-EdgeSAM, a self-prompting crack segmentation system that integrates two SOTA models, YOLOv8 and EdgeSAM, for real-time crack detection and segmentation on edge devices, such as Nvidia Orin Nano 8GB. To address the low accuracy of EdgeSAM in crack segmentation, we employed the Parameter-Efficient Fine-Tuning (PEFT) method to fine-tune EdgeSAM. Specifically, ConvLoRA weights are updated in the RepVit backbone of the image encoder, while the weights of the remaining modules are frozen during the training process. This approach enables the fine-tuned EdgeSAM to retain the original model's inference efficiency while achieving segmentation accuracy comparable to CrackSAM. To enhance the model's performance, we utilized DiceFocalLoss to minimize the potential imbalance problems during the training process. Additionally, we conducted experiments to optimize the rank parameter in the ConvLoRA method, finding that the model delivers exceptional performance when the rank equals 4. The details of our model's image encoder are summarized in TABLEV.

By comparing with the SAM-based CrackSAM and the CNN-based CrackW-net, our model presents superior processing speed and segmentation accuracy comparable to CrackSAM, achieving over four times the speed of the other two models on the same platform.

Furthermore, we briefly describe the architectural design of the climbing robot and explain the process of the automated bridge inspection tasks performed by the climbing robot.

Experimental was conducted on two bridges with different surface materials, demonstrating that the self-prompting crack segmentation system can efficiently and accurately segment cracks while the robot moves at a speed of 6.7 cm/s.

In future work, we will explore additional optimization techniques and foundational models to further enhance the system's efficiency and accuracy. Moreover, our experiments reveal that tiny cracks are challenging to detect and segment, hence, we should endeavour to develop some approaches to address this problem. For instance, we propose designating the surrounding regions of normal-sized cracks as areas of interest and applying automated up-scaling techniques to improve detection and segmentation accuracy.

REFERENCES

- [1] H. S. Munawar, A. W. A. Hammad, A. Haddad, C. A. P. Soares, and S. T. Waller. "Image-Based Crack Detection Methods: A Review," *Infrastructures*, vol. 6, no. 8, pp. 115, Aug. 2021.
- [2] D. Kang and Y.-J. Cha. "Autonomous UAVs for Structural Health Monitoring Using Deep Learning and an Ultrasonic Beacon System with Geo-Tagging," *Computer-Aided Civil and Infrastructure Engineering*, vol. 33, no. 10, pp. 885–902, May 2018.
- [3] S. Chambon and J.-M. Moliard. "Automatic Road Pavement Assessment with Image Processing: Review and Comparison," *Semantic Scholar*, pp. 1–20, 2011.
- [4] P. Subirats, J. Dumoulin, V. Legeay, and D. Barba. "Automation of Pavement Surface Crack Detection using the Continuous Wavelet Transform," in *2006 International Conference on Image Processing*, pp. 3037–3040.
- [5] S. Li, Y. Cao, and H. Cai. "Automatic Pavement-Crack Detection and Segmentation Based on Steerable Matched Filtering and an Active Contour Model," *Journal of Computing in Civil Engineering*, vol. 31, no. 5, pp. 04017045, Sep. 2017.
- [6] A. Zhang et al. "Automated Pixel-Level Pavement Crack Detection on 3D Asphalt Surfaces Using a Deep-Learning Network," *Computer-Aided Civil and Infrastructure Engineering*, vol. 32, no. 10, pp. 805–819, Aug. 2017.
- [7] W. Choi and Y.-J. Cha. "SDDNet: Real-Time Crack Segmentation," *IEEE Transactions on Industrial Electronics*, vol. 67, no. 9, pp. 8016–8025, Sept. 2020.
- [8] J. Huyan, W. Li, S. Tighe, Z. Xu, and J. Zhai. "CrackU-net: A novel deep convolutional neural network for pixelwise pavement crack detection," *Structural Control and Health Monitoring*, vol. 27, no. 8, Mar. 2020.
- [9] C. Han, T. Ma, J. Huyan, X. Huang and Y. Zhang. "CrackW-Net: A Novel Pavement Crack Image Segmentation Convolutional Neural Network," *IEEE Transactions on Intelligent Transportation Systems*, vol. 23, no. 11, pp. 22135–22144, Nov. 2022.
- [10] Z. Ye, L. Lovell, Asaad Faramarzi, and Jelena Ninić. "Sam-based instance segmentation models for the automation of structural damage detection," *Advanced Engineering Informatics*, vol. 62, pp. 102826, Sep. 2024.
- [11] K. Ge, C. Wang, Y. T. Guo, Y. S. Tang, Z. Z. Hu, and H. B. Chen. "Fine-tuning vision foundation model for crack segmentation in civil infrastructures," *Construction and Building Materials*, vol. 431, pp. 136573, May 2024.
- [12] C. Zhang et al. "A comprehensive survey on segment anything model for vision and beyond," *arXiv preprint arXiv:2305.08196*, 2023.
- [13] H. Yu, W. Yang, H. Zhang and W. He. "A UAV-based crack inspection system for concrete bridge monitoring," in *2017 IEEE International Geoscience and Remote Sensing Symposium (IGARSS)*, Fort Worth, TX, USA, pp. 3305–3308, 2017.
- [14] S. T. Nguyen and H. M. La. "A Climbing Robot for Steel Bridge Inspection," *Journal of Intelligent & Robotic Systems*, vol. 102, no. 4, Jul. 2021.
- [15] H. M. La, T. H. Dinh, N. H. Pham, Q. P. Ha, and A. Q. Pham. "Automated robotic monitoring and inspection of steel structures and bridges," *Robotica*, vol. 37, no. 5, pp. 947–967, Jan. 2018.
- [16] D. Schmidt and K. Berns. "Climbing robots for maintenance and inspections of vertical structures—A survey of design aspects and technologies," *Robotics and Autonomous Systems*, vol. 61, no. 12, pp. 1288–1305, Dec. 2013.
- [17] L. Yang et al. "Automated wall-climbing robot for concrete construction inspection," *Journal of Field Robotics*, vol. 40, no. 1, pp. 110–129, Sep. 2022.
- [18] K. Ha. "khanhha/crack_segmentation," GitHub, Feb. 21, 2024. https://github.com/khanhha/crack_segmentation
- [19] D. Guo, A. M. Rush, and Y. Kim. "Parameter-efficient transfer learning with diff pruning," *arXiv preprint arXiv:2012.07463*, 2021.
- [20] H. Neil et al. "Parameter-efficient transfer learning for NLP," in *International Conference on Machine Learning*, pp. 2790–2799, May 2019.
- [21] T. Chen et al. "SAM-Adapter: Adapting Segment Anything in Underperformed Scenes," in *2023 IEEE/CVF International Conference on Computer Vision Workshops (ICCVW)*, Paris, France, pp. 3359–3367, 2023.
- [22] E. S. Hu et al. "LoRA: Low-Rank Adaptation of Large Language Models," *arXiv preprint arXiv:2106.09685*, 2021.
- [23] Q. Zhang et al. "Adaptive Budget Allocation for Parameter-Efficient Fine-Tuning," *arXiv preprint arXiv:2303.10512*, 2023.
- [24] B. Zi, X. Qi, L. Wang, J. Wang, K.-F. Wong, and L. Zhang. "DeltaLoRA: Fine-Tuning High-Rank Parameters with the Delta of Low-Rank Matrices," *arXiv preprint arXiv:2309.02411*, 2023.
- [25] L. Q. Zhang, L. Zhang, S. Shi, X. Chu, and B. Li. "LoRA-FA: Memory-efficient Low-rank Adaptation for Large Language Models Fine-tuning," *arXiv preprint arXiv:2308.03303*, 2023.
- [26] M. Mobina, S. Shahabodini, J. Abouei, K. Arash, and A. Mohammadi. "Self-prompting polyp segmentation in colonoscopy using hybrid YOLO-SAM 2 model," *arXiv preprint arXiv:2409.09484*, 2024.
- [27] W. T. S and D. Cooke. "Robosense-Robotic delivery of sensors for seismic risk assessment," in *Proc. International Conference on Climbing and Walking Robots, CLAWAR*, pp. 847–852, 2000.
- [28] P. Sanchez-Cuevas, P. Ramon-Soria, B. Arrue, A. Ollero, and G. Heredia. "Robotic System for Inspection by Contact of Bridge Beams Using UAVs," *Sensors*, vol. 19, no. 2, pp. 305, Jan. 2019.
- [29] D. Benjumea et al. "Localization System for Lightweight Unmanned Aerial Vehicles in Inspection Tasks," *Sensors*, vol. 21, no. 17, pp. 5937, Sep. 2021.
- [30] A. Kirillov et al. "Segment Anything," in *2023 IEEE/CVF International Conference on Computer Vision (ICCV)*, Paris, France, pp. 3992–4003, 2023.
- [31] X. Zhao et al. "Fast segment anything," *arXiv preprint arXiv:2306.12156*, 2023.
- [32] Z. Chong, X. Li, C. C. Loy, and B. Dai. "EdgeSAM: Prompt-in-the-loop distillation for on-device deployment of sam," *arXiv preprint arXiv:2312.06660*, 2024.
- [33] C. Zhang et al. "Faster segment anything: Towards lightweight sam for mobile applications," *arXiv preprint arXiv:2306.14289*, 2023.
- [34] G. Jocher, A. Chaurasia, and J. Qiu. "YOLOv8 by Ultralytics," GitHub, Jan. 01, 2023. <https://github.com/ultralytics/yolov8>
- [35] S. Aleem, J. Dietlmeier, E. Arazo and S. Little. "ConvLoRA and AdaBN Based Domain Adaptation via Self-Training," in *2024 IEEE International Symposium on Biomedical Imaging (ISBI)*, Athens, Greece, pp. 1–5, 2024.
- [36] T.-Y. Lin, P. Goyal, R. Girshick, K. He and P. Dollár. "Focal Loss for Dense Object Detection," in *2017 IEEE International Conference on Computer Vision (ICCV)*, Venice, Italy, pp. 2999–3007, 2017.
- [37] F. Yang, L. Zhang, S. Yu, D. Prokhorov, X. Mei and H. Ling. "Feature Pyramid and Hierarchical Boosting Network for Pavement Crack Detection," *IEEE Transactions on Intelligent Transportation Systems*, vol. 21, no. 4, pp. 1525–1535, April 2020.
- [38] M. Eisenbach et al. "How to get pavement distress detection ready for deep learning? A systematic approach," in *2017 International Joint Conference on Neural Networks (IJCNN)*, Anchorage, AK, USA, pp. 2039–2047, 2017.
- [39] Y. Shi, L. Cui, Z. Qi, F. Meng and Z. Chen. "Automatic Road Crack Detection Using Random Structured Forests," *IEEE Transactions on Intelligent Transportation Systems*, vol. 17, no. 12, pp. 3434–3445, Dec. 2016.
- [40] R. Amhaz, S. Chambon, J. Idier and V. Baltazart. "Automatic Crack Detection on Two-Dimensional Pavement Images: An Algorithm Based on Minimal Path Selection," *IEEE Transactions on Intelligent Transportation Systems*, vol. 17, no. 10, pp. 2718–2729, Oct. 2016.
- [41] Q. Zou, Y. Cao, Q. Li, Q. Mao, and S. Wang. "CrackTree: Automatic crack detection from pavement images," *Pattern Recognition Letters*, vol. 33, no. 3, pp. 227–238, Feb. 2012.
- [42] Y. Liu, J. Yao, X. Lu, R. Xie, and L. Li. "DeepCrack: A deep hierarchical feature learning architecture for crack segmentation," *Neurocomputing*, vol. 338, pp. 139–153, Apr. 2019.